# Bis-Spiro-Oxetane and Bis-Spiro-Tetrahydrofuran Pyrroline Nitroxide Radicals: Synthesis and Electron Spin Relaxation Studies

Shengdian Huang,  $^{\dagger,a}$  Maren Pink,  $^{\S}$  Thacien Ngendahimana,  $^{\ddagger}$  Suchada Rajca,  $^{\dagger}$  Gareth R. Eaton,  $^{\ddagger}$  Sandra S. Eaton,  $^{\ddagger}$  Andrzej Rajca,  $^{\dagger}$ 

<sup>†</sup>Department of Chemistry, University of Nebraska, Lincoln, Nebraska 68588-0304

§IUMSC, Department of Chemistry, Indiana University, Bloomington, Indiana 47405-7102

<sup>‡</sup>Department of Chemistry and Biochemistry, University of Denver, Denver, CO 80208-2436

<sup>a</sup> Current address: Organix, Inc., 240 Salem Street, Woburn, MA 01801

\*Corresponding authors' E-mail addresses:

sandra.eaton@du.edu (Sandra Eaton)

arajca1@unl.edu (Andrzej Rajca)

Supporting Information Placeholder

#### At room temperature:

$$T_{\rm m}$$
 = 0.71 μs  $T_{\rm m}$  = 0.50 μs  $T_{\rm m}$  = 0.34 μs  ${\rm SSO_2Me}$   ${\rm Me}$   ${\rm Me}$ 

**ABSTRACT:** Synthesis of bis-spiro-oxetane and bis-spiro-tetrahydrofuran pyrroline nitroxide radicals relies on the Mitsunobu reaction-mediated double cyclizations of *N*-Boc protected pyrroline tetraols. Structures of the nitroxide radicals are supported by X-ray crystallography. In a trehalose/sucrose matrix at room temperature, the bis-spiro-oxetane nitroxide radical possesses electron spin coherence time,  $T_{\rm m} \approx 0.7$  µs. The observed enhanced  $T_{\rm m}$  is most likely associated with strong hydrogen bonding of oxetane moieties to the trehalose/sucrose matrix.

## Introduction

Nitroxides are stable organic radicals that have established and emerging applications in chemistry, biophysics, biomedicine, and quantum technologies. <sup>1-9</sup> One of the important applications of nitroxides in biophysics is their use as spin labels <sup>10</sup> in the site-directed spin labeling (SDSL) pulsed electron paramagnetic resonance (EPR) dipolar spectroscopy (PDS), such as double electron—electron resonance (DEER) and double quantum coherence (DQC). <sup>3,4,11</sup> These techniques are among the best for accurate measurement of the conformations of flexible regions of biomolecules. The advantages include high sensitivity, wide distance range, absolute distance distributions, and minimal structural perturbation from small-size nitroxide spin labels. <sup>4</sup>

Significant progress has been made in the design and synthesis of nitroxide spin labels to enable distance measurement with improved accuracy at physiological temperatures. The key principle is to decrease dynamic averaging effects. The common spin label, MTSL (Figure 1)<sup>12</sup> possesses two *gem*-methyl (*gem*-diMe) groups for which rotation averages inequivalent proton couplings to the unpaired electron on the timescale of the pulse EPR experiments at temperatures between about 70 and 300 K, shortening the electron spin coherence time,  $T_{\rm m}$ .  $^{13,14}$  Consequently, the PDS measurements are done at cryogenic temperatures,  $T \leq 80$  K, and preferably at T = 50 - 70 K.  $^{15,16}$ 

Recently, we and others, <sup>17-22</sup> developed spin labels devoid of the *gem*-diMe group, e.g., spiro-IA and IA-DZD (Figure 1), that enable distance measurements in proteins up to room temperature

and at  $T \approx 150$  K, respectively. <sup>17,22</sup> The distance measurements at T > 80 K were possible because replacement of methyl groups with conformationally-restricted cyclohexane rings lengthened  $T_{\rm m}$ . <sup>17-22</sup> Bis-spiro-cyclopentane pyrrolidine nitroxide (BSCPN) (Figure 1) was also prepared<sup>23</sup> and has  $T_{\rm m}$  comparable to spirocyclohexyl nitroxides. <sup>20</sup>

FIGURE 1. Spin labels and selected nitroxide radicals.

Another approach to lessen the effect of averaging inequivalent couplings of the unpaired electron to the methyl protons is demonstrated by the nitroxide structure in which the methyl groups are further away, such as in *gem-DiCarboxy-1* and -2 (Figure 1). However, only a modest increase of  $T_{\rm m}$  at room temperature was achieved.<sup>24</sup> Attaining long  $T_{\rm m}$  at room temperature is important because the longer the  $T_{\rm m}$  the greater the sensitivity of the PDS measurement, the longer the distance that can be measured, and the greater precision of the distribution of distances can be obtained.<sup>15,16</sup> In addition, radicals with long  $T_{\rm m}$  can serve as qubits.<sup>25</sup>

Motion of the nitroxide in the lattice averages g and A anisotropy and makes  $T_{\rm m}$  shorter as temperature increases, so decreasing overall mobility is an important strategy for keeping  $T_{\rm m}$  long at physiological temperatures. We are intrigued by a nitroxide radical, devoid of the gem-diMe groups, that is capable of formation of strong H-bonds with the matrix. The oxetane<sup>26-28</sup> four-membered ring ether is well-known in drug design as a much more polar replacement for a gem-diMe group.<sup>29</sup> The four-membered ring occupies a slightly smaller volume than a gem-diMe group, as indicated by comparison of the partial molar volumes in water for oxetane (61.4±0.2 cm<sup>3</sup>mol<sup>-1</sup>)<sup>30</sup> and propane (70.7±1.4 cm<sup>3</sup>mol<sup>-1</sup>),<sup>31</sup> while the five-membered tetrahydrofuran (THF) ring is slightly larger (76.7±0.2 cm<sup>3</sup>mol<sup>-1</sup>).<sup>30</sup>Replacement of a single gem-diMe group with an oxetane ring in amines decreases LogP by >1.5 units.<sup>29</sup> The bis-spiro-oxetane pyrroline nitroxide 1 is the most favorable structural motif, with the smallest molecular volume and the least hydrophobicity.

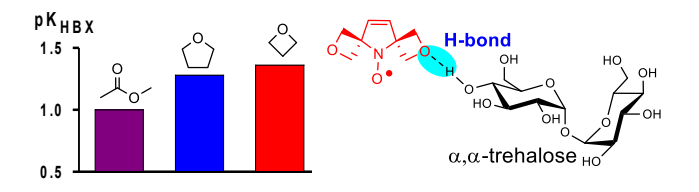


**FIGURE 2.** Values of  $pK_{HBX}$  and probable immobilization of nitroxide 1 via H-bonding in the trehalose-based matrix.

In particular, the strained C-O-C bond angle of ~90° permits the oxetane to become an excellent hydrogen-bond acceptor.

Consequently, oxetane (pK<sub>HBX</sub> = 1.36) has a higher hydrogen bonding affinity than that of THF (pK<sub>HBX</sub> = 1.28) or diethyl ether (pK<sub>HBX</sub> = 1.01).<sup>29,32,33</sup> Also, oxetane should provide much stronger hydrogen bonds than an ester, as illustrated by pK<sub>BHX</sub> = 1.00 for methyl acetate (Figure 2).<sup>33,34</sup>

We hypothesize that H-bonding between oxetane rings and hydroxyl groups of the carbohydrate matrix could reinforce immobilization of nitroxide 1, and thus contribute to increased values of  $T_{\rm m}$ . For spin labels attached to proteins, such reinforcement will contribute to lengthening the  $T_{\rm m}$  as needed for accurate, long distance measurements at physiological temperature.

We now report the synthesis of bis-spiro-cyclic nitroxide radicals 1 and 2 (Figure 1)<sup>35</sup> and their electron spin relaxation studies in a trehalose/sucrose matrix. We find that electron spin coherence times ( $T_{\rm m}$ ) are significantly longer for 1 compared to 2 or MTSL.

## **Results and Discussion**

**Synthesis.** Various synthetic methodologies for 2-oxa-5-azaspiro[3.4]octane and its derivatives have been reported, but they are not readily extendable to the bis-spirocyclic structure of  $1.^{27,28,36,37}$  Our syntheses start from *N*-Boc protected 2,5-tetrasubstituted pyrrolines 3 and  $4,^{24}$  which are reduced to the corresponding tetraols 5 and 6, using LiAlH<sub>4</sub> (Scheme 1).

**Scheme 1.** Synthesis of nitroxide radicals **1** and **2**.

The tetraols are then subjected to Mitsunobu reaction,  $^{38,39}$  providing the *N*-Boc protected bis-spirocyclic products **7** and **8** in 50+ % isolated yields for optimized reaction conditions. Deprotection of **7** gives amine **9**, which is predicted to possess relatively low basicity because each oxetane ring is expected to lower the pK<sub>a</sub> of protonated amine by about 2.7 units (assuming additivity). Nevertheless, oxidation of **7** with *m*-CPBA smoothly produces radical **1**. Deprotection of **8** cleanly gives crude TFA-salt **10**, which is then oxidized to radical **2** using the

recently developed oxidation system,<sup>22</sup> based on a modified Payne-Rosen<sup>40,41</sup> methodology.

X-ray crystallography and DFT computations. Structures of nitroxides 1 and 2 are supported by X-ray crystallography (Figure 3). The oxetane rings in 1 are slightly puckered both at 100 and 273 K, somewhat less than in parent oxetane. <sup>42</sup> The resultant  $C_2$ -symmetric chiral structure crystalizes in a chiral space group, tetragonal, P4<sub>1</sub>2<sub>1</sub>2. With the help of Cu Kα radiation, we determine the absolute structure (Flack) parameter as +0.10(3). For 2, *trans*-stereochemistry is confirmed. <sup>24</sup> THF rings are puckered, with one of the rings adopting an envelope conformation on C6 and, the other ring, a twist (half-chair) conformation on C4-C10. <sup>43</sup>  $C_1$ -symmetric 2 crystallizes in a centrosymmetric space group  $P2_1/n$ .

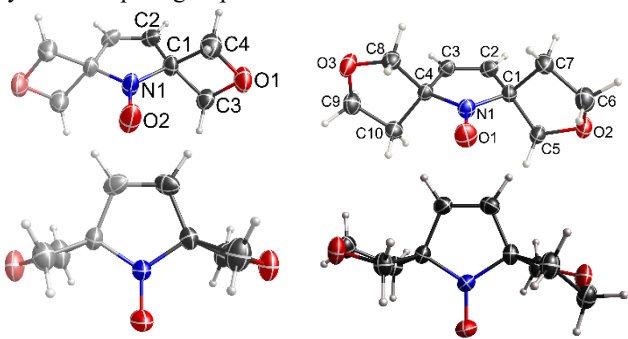


**FIGURE 3.** X-ray structures for nitroxide radicals 1 (left) and 2 (right). Carbon, nitrogen, and oxygen atoms are depicted with thermal ellipsoids set at the 50% probability level. Further details are reported in Tables S1–S12 and Figs. S1–S5, SI.

Notably, geometry optimizations, starting from X-ray determined geometries for **1** and **2**, give the corresponding  $C_{2\nu}$ - and  $C_2$ -symmetric structures at the UM06-2X/6-311+G(d,p) level in both the gas phase and PCM water solvent model. <sup>44</sup> The structures in water have nearly planar oxetane rings<sup>45</sup> and puckered (envelope) THF rings. <sup>46</sup>

**EPR and <sup>1</sup>H NMR spectroscopy of 1 and 2.** The purity of samples for nitroxides **1** and **2** was determined by paramagnetic <sup>1</sup>H NMR spectra and EPR spectroscopic spin counting. In addition, structures of the corresponding diamagnetic hydroxylamines **1-H** and **2-H**, obtained via reduction of **1** and **2** (Scheme 1), are confirmed by NMR and IR spectroscopy, and MS.

EPR spectra of nitroxides **1** and **2** in PBS buffer show triplet patterns due to isotropic <sup>14</sup>N hyperfine coupling with  $|A(^{14}N)| = 38.6$  and 42.9 MHz, respectively; *g*-values are about 2.006 (Figure 4 and Figs. S47 and S48, SI).

For 1, each of the triplet peaks is resolved into a complex multiplet, due to coupling to four and two equivalent protons with absolute values of hyperfine couplings,  $|A(^1\mathrm{H})| = 2.92$  and 1.40 MHz, respectively. In  $C_{2v}$ -symmetric 1, all four CH<sub>2</sub>-groups are equivalent, but H's within each CH<sub>2</sub>-group are diastereotopic. Consequently, the  $|A(^1\mathrm{H})| = 2.92$  MHz coupling corresponds to one of the sets with 4 equivalent protons, while the other 4-proton set remains unresolved, within the linewidth. The  $|A(^1\mathrm{H})| = 1.40$  MHz coupling is due to two equivalent vinylic protons. These assignments are confirmed by paramagnetic  $^1\mathrm{H}$  NMR and DFT computations (Table 1). In particular, the  $^1\mathrm{H}$  NMR spectrum for 1 shows three peaks at  $\delta \approx -70.6$ , -28.0, and +0.3 ppm (Figure 5), which correspond to paramagnetically shifted protons with  $A(^1\mathrm{H}) = -2.82$ , -1.28, and -0.16 MHz.

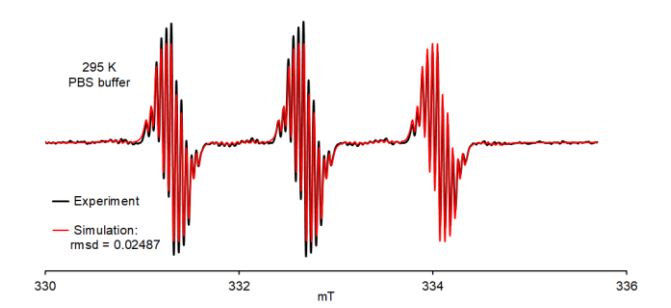


**FIGURE 4.** EPR ( $\nu$  = 9.3415 GHz) for 0.057 mM bis-spiro-oxetane nitroxide radical **1** in PBS buffer. Simulation: g = 2.0062,  $A(^{14}N)$  = 38.6 MHz (n = 1),  $A(^{1}H)$  = 2.92 MHz (n = 4),  $A(^{1}H)$  = 1.40 MHz (n = 2),  $A(^{13}C) \approx 29$  MHz (n = 4),  $A(^{13}C) \approx 25$  MHz (n = 2), peak-to-peak linewidths, Gaussian = 0.0010 mT and Lorentzian = 0.033 mT (all nuclei are at natural abundance).

**TABLE 1.** Experimental and DFT-Computed Isotropic <sup>1</sup>H Hyperfine Couplings ( $A(^{1}H)$  in MHz) for Nitroxide Radicals. <sup>a</sup>

	vinylic			O-CH <sub>2</sub> -C			C-CH <sub>2</sub> -C	
	EPR	NMR	DFT	EPR	NMR	DFT	NMR	DFT
1	1.40	-1.28	-1.73	2.92	-2.82	-2.77	-	-
					-0.16	-0.11		
2	-	-1.14	-1.73	-	-2.45	-2.71		
					-0.18	-1.62	-0.86	-2.47
					+1.76	+2.55	+0.02	-0.38
					+1.15	+0.09		

<sup>a</sup> Computations: UM06-2X/EPR-III///UM06-2X/6-311+G(d,p) + ZPVE in water PCM solvent model. NMR-derived values of  $A(^{1}H)$  are not corrected for bulk magnetic susceptibility shifts.

For  $C_2$ -symmetric **2**, there are 7 distinct sets of 2 equivalent (homotopic) protons, corresponding to the vinylic H's and diastereotopic H's within each pair of homotopic CH<sub>2</sub> groups. Although, the EPR spectrum of **2** does not show resolved <sup>1</sup>H hyperfine couplings (Fig. S48, SI), in paramagnetic <sup>1</sup>H NMR, seven distinct peaks are observed (Figure 5).

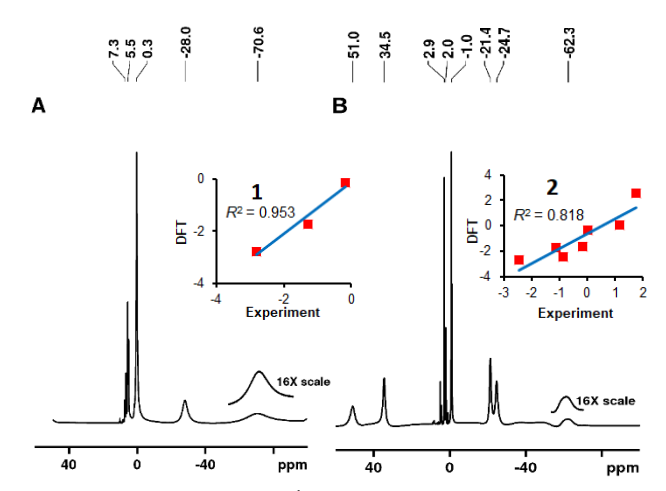


**FIGURE 5.** Paramagnetic <sup>1</sup>H NMR (400 and 700 MHz, +60 to - 100 ppm range) spectra of nitroxide radicals: **A**, 1.3 M **1** in chloroform-d and **B**, 0.86 M **2** in acetone- $d_6$ . Peaks at 7.3 and 2.0 ppm correspond to residual solvent peaks. Inset plots: correlation between DFT-computed and experimental values of  $A(^1\text{H})$ .

Notably, all  $A(^{1}\mathrm{H}) < 0$  are observed in 1, but in 2, diastereotopic protons within one pair of homotopic CH<sub>2</sub> groups have two values of  $A(^{1}\mathrm{H}) > 0$ , in agreement with a qualitative spin polarization mechanism for delocalization of spin density.<sup>47</sup> Peak assignments for both 1 and 2 are aided by correlations, between the values of  $A(^{1}\mathrm{H})$  obtained from DFT computations and paramagnetic  $^{1}\mathrm{H}$  NMR shifts, with  $R^{2}=0.953$  and 0.818, respectively (Table 1, Figure 5, and Fig. S38, SI).<sup>43</sup>

**Electron spin relaxation.** We have reported  $T_{\rm m}$  values for several new spin labels and spin-labeled proteins over the past several years.  $^{17,18,21,22}$  Here we report results obtained with stretched exponentials which, compared to single exponential fits, give better fits to the echo dephasing curves. In addition, the stretch parameter,  $\beta$ , is a useful indicator of mobility. The disadvantage of the stretch exponential fits is that by having two adjustable parameters,  $T_{\rm m}$  and  $\beta$ , there is more scatter in the resulting values of  $T_{\rm m}$ .

The temperature dependence of the relaxation rate,  $1/T_m$ , in 9:1 trehalose/sucrose indicates that nitroxide radical 1 is by far the slowest relaxing, especially at T > 200 K (Figure 6).

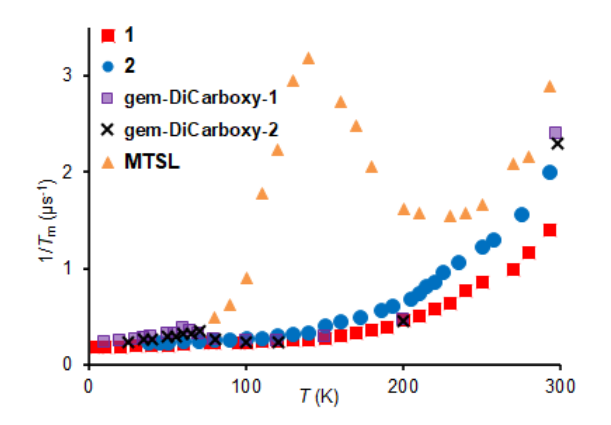


**FIGURE 6.** Temperature dependence of  $1/T_m$  at X-band (9.44 GHz) in the perpendicular plane in 9:1 trehalose/sucrose matrix.

At room temperature,  $T_{\rm m}=0.71,\,0.50,\,0.42,\,0.44,\,{\rm and}\,0.34\,\,{\rm \mu s}$  are found for 1, 2, gem-DiCarboxy-1 and -2, and MTSL nitroxide radicals, respectively. As discussed before,  $^{13,14,18}$  gem-diMebased nitroxide radicals, such as MTSL, have pronounced maxima in the relaxation rate at about  $T\approx 140$  K, associated with the methyl group rotation. Relative values of the stretch parameters  $\beta$  at T<200 K are 1>2> MTSL (Fig. S50, SI), thus suggesting superior immobilization of 1 in a trehalose/sucrose matrix.

## Conclusion

We have synthesized the first nitroxide radicals containing bisspiro-oxetane and -THF moieties. The key step in the synthesis relies on the Mitsunobu reaction-mediated double cyclizations of N-Boc protected pyrroline tetraols. In a trehalose/sucrose matrix, bis-spiro-oxetane nitroxide radical 1 possesses electron spin coherence time,  $T_{\rm m}\approx 0.7~\mu \rm s$ , at room temperature, compared to  $T_{\rm m}\approx 0.5$  and 0.34  $\mu \rm s$  for 2 and MTSL, respectively. We attribute the enhanced  $T_{\rm m}$  for 1 with strong hydrogen bonding of oxetane moieties to the trehalose-based matrix.

#### **Experimental Section**

General Section. Standard techniques for synthesis under inert atmosphere (argon or nitrogen), using custom-made Schlenk glassware and custom-made double manifold high vacuum lines, were employed. Tetrahydrofuran (THF) was freshly distilled from sodium/benzophenone prior to use. Other solvents, e.g., dichloromethane (DCM) or toluene, were used directly from a commercial solvent purification system. Chromatographic separations were carried out using normal phase neutral alumina (32-63 μm) or silica gel (60 Å, 40-75 μm).

NMR spectra were obtained using commercial spectrometers (1H, 400, 600, and 700 MHz) with chloroform-d (CDCl<sub>3</sub>), acetone- $d_6$ , methanol- $d_4$  (CD<sub>3</sub>OD), or DMSO- $d_6$ , as solvent. The 700 MHz instrument was equipped with a cryoprobe. The chemical shift references were as follows: (1H) chloroform-h, 7.26 ppm; ( $^{13}$ C) chloroform-d, 77.2 ppm; ( $^{1}$ H) acetone-d<sub>5</sub>, 2.05 ppm; ( $^{13}$ C) acetone- $d_6$ , 30.2 ppm; ( $^{1}$ H) methanol- $d_3$ , 3.31 ppm; ( $^{13}$ C) methanol- $d_4$ , 49.3 ppm; ( $^{1}$ H) DMSO- $d_5$ , 2.50 ppm; ( $^{13}$ C) DMSO- $d_6$ , 39.5 ppm. Typical 1D FID was subjected to exponential multiplication with an exponent of 0.1 Hz (for <sup>1</sup>H) and 1.0-2.0 Hz (for  $^{13}$ C). It should be noted that NMR spectra of N-Boc-protected pyrrolines show additional resonances because of the presence of two diastereomers arising due to slow rotation (on the NMR time scale) about the carbamate C-N bond. IR spectra were obtained using a commercial instrument, equipped with an ATR sampling accessory. MS analyses were carried out at local facilities for mass spectrometry.

**Synthesis of starting materials.** Starting materials, *N*-Boc protected 2,5-tetrasubstituted pyrrolines **3** and **4**, were prepared according to the literature procedures.<sup>24</sup>

Typical procedures for products. General procedure for tetraols 5 and 6. The starting material (3 or 4, 1 equiv) and THF (ca. 12 mL, to make 0.04 - 0.1 M solution of 3 or 4) were added to a Schlenk reactor and cooled in an ice water bath. Lithium aluminum hydride (5 equiv) was added in one portion with stirring, to produce a grey slurry. The reaction mixture was stirred for five minutes at 0 °C, and then for overnight at room temperature. Subsequently, the mixture was diluted with an equal volume of ether, quenched with water (ca. 10 equiv) at 0 °C, followed by the addition of equal volume of 10% NaOH solution (equal to 10 equiv of water), and then, after stirring for 15 min, an extra portion of water (ca. 30 equiv) was added and the reaction mixture was removed from ice bath. Magnesium sulfate was added to the mixture and following stirring at room temperature for 30 min, the salts were filtered off and the organic layer was dried over sodium sulfate. The solvents were removed on rotatory evaporator to produce crude product which was purified by column chromatography (silica gel, dichloromethane/acetone, 1:1 or 1:2).

**5** white solid (213.1 mg, 46%).  $R_{\rm f} = 0.34$  in dichloromethane/acetone, 1:3. Mp: 165–167 °C. <sup>1</sup>H NMR (400 MHz, CD<sub>3</sub>OD):  $\delta$  5.74 (s, 2 H), 4.15 (d, J = 10.8 Hz, 2H), 3.98 (d, J = 10.8 Hz, 2H), 3.61 (dd, J = 10.8 Hz, 4.0 Hz, 4H), 1.51 (s, 9 H). <sup>13</sup>C { <sup>1</sup>H } NMR (400 MHz, CD<sub>3</sub>OD):  $\delta$  154.9, 133.4, 132.9, 82.3, 79.2, 78.3, 63.9, 63.2, 29.1. TOF-HRMS-EI (1% CH<sub>3</sub>COONa in 3:1 (v/v) MeOH/H<sub>2</sub>O): Calcd. for C<sub>13</sub>H<sub>24</sub>NO<sub>6</sub> at [M+H] <sup>+</sup>: 290.1604; found: 290.1610 (2.1 ppm). IR (diamond, cm<sup>-1</sup>): 3248, 1691, 1391, 1363, 1314, 1175, 1112, 1064, 992, 851, 778.

**6** white solid (108.84 mg, 73%).  $R_{\rm f} = 0.23$  in dichloromethane/acetone, 1:3. Mp: 93–95 °C. ¹H NMR (400 MHz, DMSO- $d_6$ ):  $\delta$  5.66 (d, J = 6.3 Hz, 1H), 5.61 (d, J = 6.3 Hz, 1H),

4.92 (t, J = 5.2 Hz, 1H), 4.83 (t, J = 5.2, 1H), 4.46 (t, J = 4.9 Hz, 1H), 4.41 (t, J = 4.9 Hz, 1H), 3.62 (bs, 3H), 3.51 (m, 1H), 3.38 (s, 2H), 3.37 (s, 2H), 3.34 (s, H<sub>2</sub>O in DMSO- $d_6$ ), 2.11 (m, 1H), 2.05 (m, 1H), 1.98 (m, 1H), 1.84 (m, 1H), 1.40 (s, 9 H).  $^{13}$ C { $^{1}$ H} NMR (176 MHz, DMSO- $d_6$ ):  $\delta$  152.7, 131.52, 131.02, 78.7, 74.5, 73.7, 66.2, 65.2, 57.6, 37.1, 36.2, 28.2. TOF-HRMS-EI (1% CH<sub>3</sub>COONa in 3:1 (v/v) MeOH/H<sub>2</sub>O): Calcd. for C<sub>15</sub>H<sub>27</sub>NNaO<sub>6</sub> at [M+Na]<sup>+</sup>: 340.1731; found: 340.1732 (0.3 ppm). IR (diamond, cm<sup>-1</sup>): 3169, 1683, 1641, 1455, 1389, 1375, 1365, 1331, 1256, 1177, 1154, 1098, 1082, 1059, 1042, 1016, 1006, 977, 936, 852, 773, 760, 745.

General procedure for 7 and 8 (Mitsunobu reaction). The starting material 5 (97 mg, 0.36 mmol, 1 equiv) or 6 (60 mg, 0.19 mmol, 1 equiv) and triphenylphosphine (352 mg, 1.34 mmol, 3.7 equiv for **5**) or (198.5 mg, 0.76 mmol, 4.0 equiv for **6**) were added to a Schlenk reactor that was evacuated overnight then filled with nitrogen before adding toluene (10 mL for 5) or (6 mL for 6). To the resulting solution was added neat diethyl azodicarboxylate (233.7 mg, 210 µL, 1.34 mmol, 3.7 equiv for 5) or as a 40% v/v solution in toluene (0.3 mL, 0.76 mmol, 4.0 equiv for 6). The Schlenk reactor was moved to an oil bath, to allow the reaction to stir at 80 °C for 24 h for 5 or 12 h for 6. The reaction solution turned from pale yellow to orange or to deep red immediately in the oil bath. To obtain the crude product 7, the reaction mixture was quenched with water and extracted with ethyl acetate (15 x 3 mL); then, the organic layers were collected and dried over Na<sub>2</sub>SO<sub>4</sub>, and finally concentrated. For 8, the crude product was obtained by removing toluene. The crude products were purified with column chromatography (silica gel, pentane/acetone, 15:1 or 20:1).

7 white solid (50.0 mg, 63%).  $R_{\rm f}$ = 0.68 in pentane/acetone, 2:1). Mp: 113–116 °C. ¹H NMR (400 MHz, CDCl<sub>3</sub>):  $\delta$  6.18 (s, 2 H), 5.46 (s, 2H), 5.26 (s, 2H), 4.51 (s, 4H), 1.64 (s, 9 H). ¹³C {¹H} NMR (400 MHz, CDCl<sub>3</sub>):  $\delta$  152.8, 131.1, 81.87, 81.48, 79.84, 70.4, 69.4, 28.7. TOF-HRMS-EI (1% CH<sub>3</sub>COONa in 3:1 (v/v) MeOH/H<sub>2</sub>O): Calcd. for C<sub>13</sub>H<sub>19</sub>NO<sub>4</sub>Na at [M+Na]<sup>+</sup>: 276.1212; found: 276.1213 (0.4 ppm). IR (diamond, cm⁻¹): 2970, 2938, 2873, 1690, 1480, 1453, 1380, 1361, 1287, 1243, 1168, 1112, 1050, 978, 911, 847, 818, 765, 745.

**8** white solid (21.3 mg, 40%).  $R_f$  = 0.74 in pentane/acetone, 5:1. Mp: 60–61 °C. ¹H NMR (400 MHz, CDCl<sub>3</sub>):  $\delta$  5.72 (s, 2H), 4.18 (bs, 2H), 4.06 (bs, 2H), 3.94 (m, 2H), 3.57 (d, J = 8.4 Hz, 2H), 2.58 (bs, 1H), 2.51 (bs, 1H), 1.84 (bs, 2H), 1.52 (s, 9 H).  $^{13}$ C { $^{1}$ H} NMR (100 MHz, CDCl<sub>3</sub>):  $\delta$  152.1, 131.4, 80.9, 76.3, 75.26, 75.09, 73.9, 69.08, 68.74, 68.24 (impurity), 37.4, 36.6, 28.9. TOF-HRMS-EI (1% CH<sub>3</sub>COONa in 3:1 (v/v) MeOH/H<sub>2</sub>O): Calcd. for C<sub>15</sub>H<sub>23</sub>NNaO<sub>4</sub> at [M+Na]<sup>+</sup>: 304.15193; found: 304.15199 (0.2 ppm). IR (diamond, cm<sup>-1</sup>): 1691, 1460, 1377, 1363, 1255, 1161, 1102, 1071, 1031, 971, 941, 915, 843, 772, 659.

General procedure for 9 and 10 (Boc deprotection). The starting material 7 (50.1 mg, 0.198 mmol for 7) or 8 (24.0 mg, 0.085 mmol) and dichloromethane (2.0 mL for 7) or (0.5 mL for 8) were added to a round bottom flask and cooled in an ice water bath. For 7, trifluoroacetic acid (0.15 mL, 1.98 mmol) was added dropwise and then the solution was stirred for five minutes after which the ice water bath was removed. The solution was stirred for three hours until the starting material could not be observed by thin layer chromatography. The macroporous polystyrene (MP) triethylamine resin (loading: 3.8 mmol/g, 0.6 g) was added to the reaction and the mixture was stirred at room temperature for another 1 h. The resin was

filtered off, and the organic solvent was collected and concentrated to afford the crude product 9. The crude product was purified by column chromatography (silica gel, pentane/acetone, 3:1). For 8, trifluoroacetic acid (130.6  $\mu L$ , 1.7 mmol) was dissolved in 1.0 mL of dichloromethane and half of this solution was added to the flask containing 8. The reaction was stirred at room temperature for 1 h after the ice water bath had been removed. After 1 h at room temperature, the starting material could not be observed by thin layer chromatography. The dichloromethane and trifluoroacetic acid were evaporated on a rotary evaporator. The resulting brown oil was dissolved in methanol (2 mL) and evaporated three times to yield the crude product, which was directly used in the next step.

**9** white solid (12.6 mg, 42%).  $R_f$  = 0.15 in pentane/ethyl acetate, 2:1. Mp: 108–110 °C. ¹H NMR (400 MHz, CDCl<sub>3</sub>):  $\delta$  8.92 (s, 1H), 6.24 (s, 2 H), 4.99 (d, J = 7.6 Hz, 4H), 4.71 (d, J = 7.6 Hz, 4H).  $^{13}$ C{ $^{1}$ H} NMR (400 MHz, CDCl<sub>3</sub>):  $\delta$  131.4, 80.9, 71.2. TOF-HRMS-EI (1% CH<sub>3</sub>COONa in 3:1 (v/v) MeOH/H<sub>2</sub>O; ion type, % RA for m/z): Calcd. for C<sub>8</sub>H<sub>11</sub>NO<sub>2</sub> at [M]<sup>+</sup>: 153.0790; found: 153.0796 (4.1 ppm). IR (diamond, cm<sup>-1</sup>): 3332, 2944, 2866, 1444, 1226, 1163, 974, 962, 899, 762.

**10** brown solid (23.3 mg). Mp: 175–177 °C. <sup>1</sup>H NMR (400 MHz, CDCl<sub>3</sub>):  $\delta$  5.83 (s, 2 H), 4.34 (d, J = 10.8 Hz, 2H), 4.11 (m, 2H), 3.98 (m, 2H), 3.76 (d, J = 10.4 Hz, 2H), 2.72 (m, 2H), 2.22 (m, 2H). <sup>13</sup>C{<sup>1</sup>H} NMR (176 MHz, CDCl<sub>3</sub>):  $\delta$  161.6 [J (<sup>13</sup>C-<sup>19</sup>F) = 37.5 Hz], 130.4, 78.9, 74.4, 67.9, 37.1. <sup>19</sup>F NMR (376 MHz, CDCl<sub>3</sub>):  $\delta$  –75.8. TOF-HRMS-EI (1% CH<sub>3</sub>COONa in 3:1 (v/v) MeOH/H<sub>2</sub>O): Calcd. for C<sub>10</sub>H<sub>15</sub>NNaO<sub>2</sub> at [M+Na]<sup>+</sup>: 204.0995; found: 204.0994 (0.5 ppm). IR (diamond, cm<sup>-1</sup>): 2877, 1659, 1620, 1478, 1463, 1431, 1201, 1175, 1136, 1085, 1047, 959, 929, 912, 835, 798, 761, 721.

Procedure for nitroxide radical 1. The starting material 9 (12.6 mg, 0.08 mmol) was added to a Schlenk reactor and was dissolved in dichloromethane (0.8 mL). The resulting solution was added to a solution of m-CPBA (28.4 mg, 0.16 mmol) in dichloromethane (1.2 mL) dropwise. The resulting solution was stirred for 15 minutes, then the ice bath was removed. The reaction was stirred at room temperature for 4 h until the starting material could not be observed by thin layer chromatography. The reaction was diluted with ether (5 mL), washed with Na-HCO<sub>3</sub> solution, and then washed with brine. The organic layer was collected and dried over NaSO<sub>4</sub>. The solvent was evaporated to give pale yellow powdery crude product. The crude product was purified with column chromatography (silica gel, pentane/ethyl acetate, 3:1) to afford nitroxide radical 1 as a yellow solid (5.4 mg, 39.1%).  $R_f = 0.35$  in pentane/acetone, 2:1). Mp: 88–90 °C. EPR (X-band, 0.64 mM in CHCl<sub>3</sub>), spin concentration = 95%. TOF-HRMS-EI (1% CH<sub>3</sub>COONa in 3:1 (v/v) MeOH/H<sub>2</sub>O): Calcd. for C<sub>8</sub>H<sub>10</sub>NO<sub>3</sub> at [M]<sup>+</sup>: 168.0661; found: 168.0660 (0.4 ppm). IR (diamond, cm<sup>-1</sup>): 3065, 2945, 2874, 1724, 977, 923, 772.

<u>Procedure for nitroxide radical 2.</u> The starting material **10** was evenly divided into 2 vials with each containing 25.8 mg (0.087 mmol). To each vial was added NaHCO<sub>3</sub> (27.7 mg, 0.332 mmol), NaWO<sub>4</sub>·2H<sub>2</sub>O (4.3 mg, 0.0131 mmol), MeOH (0.77 mL), and PhCN (109  $\mu$ L). At 0 °C, H<sub>2</sub>O<sub>2</sub> (35 wt. %, 154  $\mu$ L) was added dropwise. The reactions were stirred vigorously with protection from light at room temperature for 6.5 h. After 6.5 h, the solvents in the two vials were removed by nitrogen gas to afford the crude as a mixture of white and yellow solid. The solids from the two vials were combined and crude was purified

on neutral aluminum oxide chromatography (pentane/ethyl acetate, 3:1;  $R_f$  = 0.38 in pentane/ethyl acetate, 1:1 on neutral aluminum oxide TLC) to yield the nitroxide **2** as a yellow solid (2 reactions, total 25.8 mg). Mp: 60–62 °C. EPR (X-band, 2.19 mM in benzene), spin concentration = 99.7%  $\approx$  100%. TOF-HRMS-EI (1% CH<sub>3</sub>COONa in 3:1 (v/v) MeOH/H<sub>2</sub>O): Calcd. for C<sub>10</sub>H<sub>14</sub>NNaO<sub>3</sub> at [M+Na]<sup>+</sup>: 219.0866; found: 219.0868 (1.1 ppm). IR (diamond, cm<sup>-1</sup>): 2826, 1422, 1363, 1259, 1224, 1061, 969, 947, 922, 900, 858, 765, 727.

# General procedure for 1-H and 2-H (reduction of nitroxides).

1-H (Label: HSD-5-85): Nitroxide radical 1 (10.1 mg, 0.0601 mmol, 1.0 equiv) or 2 (5.0 mg, 0.0255 mmol, 1.0 equiv) was added to 1.5 ml of phosphate buffered saline (PBS; 12.4 mM for 1 and 50 mM for 2), and then sonicated to give a cloudy solution. To this solution, L-ascorbic acid (5.0 equiv) was added. The mixture was stirred at ambient temperature with protection from light. After 3 h, the solution was extracted with ethyl acetate (3 x 3 mL), and the organic layer was dried over Na<sub>2</sub>SO<sub>4</sub>. The solvent was evaporated to give the crude product, which, for 1-H, was then purified with column chromatography (silica gel, pentane/acetone, 2:1), to afford the hydroxylamine.

**1-H** white solid (7.0 mg, 68.8%).  $R_{\rm f} = 0.32$  in pentane/acetone, 2:1. Mp: 107–110 °C. ¹H NMR (400 MHz, CDCl<sub>3</sub>):  $\delta$  6.21 (s, 2 H), 5.01 (d, J = 6.8 Hz, 4H), 4.57 (d, J = 6.8 Hz, 4H). ¹³C {¹H} NMR (176 MHz, CDCl<sub>3</sub>):  $\delta$  131.3, 77.9, 73.2. TOF-HRMS-EI (1% CH<sub>3</sub>COONa in 3:1 (v/v) MeOH/H<sub>2</sub>O; ion type, % RA for m/z): Calcd. for C<sub>8</sub>H<sub>12</sub>NO<sub>3</sub> at [M+H]<sup>+</sup>: 170.0817; found: 170.0814 (-1.8 ppm). IR (diamond, cm⁻¹): 3281, 2949, 2867, 1449, 1367, 1234, 1197, 1054, 1023, 975, 965, 944, 924, 858, 809, 757, 712.

**2-H** colorless oil. <sup>1</sup>H NMR (400 MHz, acetone- $d_6$ ):  $\delta$  7.10 (s, 0.5H), 5.81 (s, 2H), 3.94 (d, J = 8.8 Hz, 2H,  ${}^{1}H^{-1}H$  COSY crosspeak to <sup>1</sup>H 3.46 ppm), 3.78 (m, 2H, <sup>1</sup>H-<sup>1</sup>H COSY cross-peak to <sup>1</sup>H 2.28 and 1.71 ppm), 3.72 (m, 2H, <sup>1</sup>H-<sup>1</sup>H COSY cross-peak to  ${}^{1}\text{H}$  2.28 and 1.71 ppm), 3.46 (d, J = 9.2 Hz, 2H,  ${}^{1}\text{H}$ - ${}^{1}\text{H}$  COSY cross-peak to  ${}^{1}\text{H}$  3.94 ppm), 2.28 (dt, J = 11.6, 6.4 Hz, 2H,  ${}^{1}\text{H}$ -<sup>1</sup>H COSY cross-peaks to <sup>1</sup>H 3.70-3.82 ppm and 1.71 ppm), 1.71 (dt, J = 12.4, 7.2 Hz, 2H, <sup>1</sup>H-<sup>1</sup>H COSY cross-peaks to <sup>1</sup>H 3.70-3.82 ppm and 2.28 ppm). <sup>13</sup>C{<sup>1</sup>H} NMR (100 MHz, acetone $d_6$ ):  $\delta$  134.1 (<sup>1</sup>H-<sup>13</sup>C HSQC cross-peak to <sup>1</sup>H 5.81 ppm), 79.9, 74.0 (<sup>1</sup>H-<sup>13</sup>C HSQC cross-peak to <sup>1</sup>H 3.94 and 3.46 ppm), 69.3 (1H-13C HSQC cross-peak to 1H 3.70-3.82 ppm), 36.9 (1H-13C HSQC cross-peak to <sup>1</sup>H 2.28 and 1.71 ppm). TOF-HRMS-EI (1% CH<sub>3</sub>COONa in 3:1 (v/v) MeOH/H<sub>2</sub>O): Calcd. for  $C_{10}H_{15}NNaO_3$  at  $[M+Na]^+$ : 220.0944; found: 220.0953 (3.6) ppm). IR (diamond, cm<sup>-1</sup>): 3330, 2856, 1434, 1359, 1222, 1100, 1047, 972, 912, 850, 753.

**X-ray crystallography.** For nitroxide radicals 1 and 2, the structures were determined using crystals obtained by slow evaporation of DCM/pentane solution and slow evaporation of ethyl acetate/pentane solution, respectively. Structures of 1 were determined using Mo Kα radiation at 296 K and 100 K, and Cu Kα radiation at 273 K and 100 K. The longer wavelength radiation (Cu Kα) was employed to determine unequivocally crystal chirality. As expected, at lower temperatures oxetane rings are slightly more puckered. Structure of **2** was determined using Mo Kα radiation at 173 K. Further details, including the data acquisition and refinement are described in the SI and the deposited cif files.

**EPR spectroscopy.** Variable temperature  $T_1$  and  $T_m$  were recorded using a commercial spectrometer (model E580) equipped

with an ER4118X-MS5 split ring resonator. Temperatures between 10 and 70 K were achieved with a commercial closedcycle system and temperatures above 70 K were attained with a commercial liquid nitrogen flow system. Temperature was monitored with a calibrated cernox sensor located close to the resonator. The sample temperature was estimated to be accurate to ~1 K.  $T_{\rm m}$  was calculated from two pulse echo decays ( $\pi/2$ - $\tau$ - $\pi$ - $\tau$ -echo) obtained with a  $\pi/2$  pulse length of 20 ns and an initial  $\tau$  value of 200 ns. The microwave power, gain, and scans averaged were adjusted to maximize the echo and improve the signal to noise. The decay curves were fitted with single exponentials or a stretched exponential. At lower temperature temperatures the echo dephasing is dominated by nuclear spin diffusion<sup>14</sup> and a stretched exponential is required to fit the shape of the decay curves. As temperature is increased and motion increases, the value of the stretch parameter  $\beta$  decreases (Fig. S50, SI). When  $\beta$  equals 1, the stretched exponential function is identical to a single exponential. When fitting to a stretched exponential results in values of  $\beta$  that are close to 1, the fit functions for the stretched exponential and a single exponential are very similar and there is greater relative uncertainty in the value of  $\beta$ than for larger values of  $\beta$ . Comparison of the temperature dependence of  $1/T_{\rm m}$  for 1 and 2 with that for MTSL, calculated using a stretched exponential is presented in Figure 6. If  $\beta$  is not 1, the selection of a fitting function impacts the value of  $T_{\rm m}$ . Values of  $T_{\rm m}$  for 1, 2, and MTSL from ~230 K up to room temperature are shown in Fig. S51, SI for both a single exponential and a stretched exponential. Independent of fit function, the values of  $T_m$  in 9:1 trehalose: sucrose decrease in the order 1 > 2 >MTSL. Further details, including determination of  $T_1$  temperature dependence and its modelling, and CW EPR spectroscopic studies are described in the SI.

Computational methods. Ground-state geometries of nitroxide radicals were optimized at the UM06-2X/6-311+G(d,p)+ZPVE and UB3LYP/6-311+G(d,p)+ZPVE levels in the gas phase and using default Gaussian 16 water solvent model (Table S14, SI).<sup>44</sup> When starting the geometry optimization of nitroxide radicals 1 and 2 with an X-ray structure determined  $C_2$ - and  $C_1$ -symmetric conformation,  $C_2$ - and  $C_2$ -symmetric structures, respectively, as minima on potential energy surface (PES). For 2, THF rings adopt envelopes on C (equivalent to C6 and C9 in the X-ray structure in Figure 3) conformation (Table S15, SI). Further details may be found in the SI.

# **ASSOCIATED CONTENT**

## Supporting Information

The Supporting Information is available free of charge on the ACS Publications website.

<sup>1</sup>H, <sup>13</sup>C, <sup>19</sup>F NMR, and IR spectra, and HR MS of products; experimental information, including summaries for each synthetic step, X-ray crystallography, and EPR spectroscopy; computational details (PDF)

## **Accession Codes**

CCDC nos: 2084248 (1), 2084249 (1), 2084250 (1), 2084251 (1), and 2084252 (2) contain the supplementary crystallographic data for this paper. These data can be obtained free of charge via <a href="https://www.ccdc.cam.ac.uk/data\_request/cif">www.ccdc.cam.ac.uk/data\_request/cif</a>, or by emailing <a href="https://data\_request/cif">data\_request/cif</a>, or by contacting The Cambridge Crystallographic Data Centre, 12 Union Road, Cambridge CB2 1EZ, UK; <a href="https://dax:+441223336033">fax:+441223336033</a>.

#### **AUTHOR INFORMATION**

## Corresponding Authors: Orcid Links:

Sandra S. Eaton – <a href="https://orcid.org/0000-0002-2731-7986">https://orcid.org/0000-0002-2731-7986</a>
Andrzej Rajca – <a href="https://orcid.org/0000-0002-8856-1536">https://orcid.org/0000-0002-8856-1536</a>

#### Authors: Orcid Links:

 $\label{eq:control_co$ 

#### **Author Contributions**

The manuscript was written through contributions of all authors. All authors have given approval to the final version of the manuscript.

#### Notes

The authors declare no competing financial interest.

## Acknowledgment

Support of this research by the National Institutes of Health (NIGMS R01GM124310-01 to AR, SR, and SSE) and the Chemistry Division of the National Science Foundation (CHE-1955349 to AR) is gratefully acknowledged. Support for the acquisition of the Bruker Venture D8 diffractometer through the Major Scientific Research Equipment Fund from the President of Indiana University and the Office of the Vice President for Research is gratefully acknowledged.

#### References

- (1) Tebben, L.; Studer, A. Nitroxides: Applications in Synthesis and in Polymer Chemistry. *Angew. Chem.*, *Int. Ed.* **2011**, *50*, 5034–5068.
- (2) Nutting, J. E.; Rafiee, M.; Stahl, S. S. Tetramethylpiperidine N-Oxyl (TEMPO), Phthalimide N-Oxyl (PINO), and Related N-Oxyl Species: Electrochemical Properties and Their Use in Electrocatalytic Reactions. *Chem. Rev.* **2018**, *118*, 4834–4885.
- (3) Hubbell, W. L.; Lopez, C. J.; Altenbach, C.; Yang, Z. Technological Advances in Site-Directed Spin Labeling of Proteins. *Curr. Opin. Struct. Biol.* **2013**, *23*, 725–733.
- (4) Haugland, M. M.; Lovett, J. E.; Anderson, E. A. Advances in the Synthesis of Nitroxide Radicals for Use in Biomolecule Spin Labelling. *Chem. Soc. Rev.* **2018**, *47*, 668–680.
- (5) (a) Rajca, A.; Wang, Y.; Boska, M.; Paletta, J. T.; Olankitwanit, A.; Swanson, M. A.; Mitchell, D. G.; Eaton, S. S.; Eaton, G. R.; Rajca, S. Organic Radical Contrast Agents for Magnetic Resonance Imaging. *J. Am. Chem. Soc.* **2012**, *134*, 15724–15727. (b) Nguyen, H. V. T.; Chen, Q.; Paletta, J. T.; Harvey, P.; Jiang, Y.; Zhang, H.; Boska, M. D.; Ottaviani, M. F.; Jasanoff, A.; Rajca, A.; Johnson, J. A. Nitroxide-based macromolecular contrast agents with unprecedented transverse relaxivity and stability for magnetic resonance imaging of tumors. *ACS Central Science* **2017**, *3*, 800–811.
- (6) Matsumoto, K.; Mitchell, J. B.; Krishna, M. C. Multimodal Functional Imaging for Cancer/Tumor Microenvironments Based on MRI, EPRI, and PET. *Molecules* **2021**, *26*, 1614 (1-27).
- (7) Herrmann, C.; Solomon, G. C.; Ratner, M. A. Organic Radicals as Spin Filters. J. Am. Chem. Soc. 2010, 132, 3682–3684.
- (8) Gallagher, N.; Olankitwanit, A.; Rajca, A. High-Spin Organic Molecules. *J. Org. Chem.* **2015**, *80*, 1291–1298.
- (9) Shu, C.; Pink, M.; Junghoefer, T.; Nadler, E.; Rajca, S.; Casu, M. B.; Rajca, A. Synthesis and Thin Films of Thermally Robust Quartet (*S* = 3/2) Ground State Triradical. *J. Am. Chem. Soc.* **2021**, *143*, 5508–5518.

- (10) Stone, T. J.; Buckman, T.; Nordio, P. L.; McConnell, H. M. Spin-labeled biomolecules. *Proc. Natl. Acad. Sci. U. S. A.* **1965**, *54*, 1010–1017.
- (11) Borbat, P. P.; Costa-Filho, A. J.; Earle, K. A.; Moscicki, J. K.; Freed, J. H. Electron spin resonance in studies of membranes and proteins. *Science* **2001**, *291*, 266–269.
- (12) Berliner, L. J.; Grunwald, J.; Hankovszky, H. O.; Hideg, K. A Novel Reversible Thiol Specific Spin Label: Papain Active Site Labeling and Inhibition. *Anal. Biochem.* **1982**, *119*, 450–455.
- (13) Dzuba, S. A.; Maryasov, A. G.; Salikhov, K. M.; Tsvetkov, Yu. D. Superslow rotations of nitroxide radicals studied by pulse EPR spectroscopy. *J. Magn. Reson.* **1984**, *58*, 95–117.
- (14) Zecevic, A.; Eaton, G. R.; Eaton, S. S.; Lindgren, M. Dephasing of electron spin echoes for nitroxyl radicals in glassy solvents by nonmethyl and methyl protons. *Mol. Phys.* **1998**, *95*, 1255–1263.
- (15) Jeschke, G. DEER Distance Measurements on Proteins. *Annu. Rev. Phys. Chem.* **2012**, *63*, 419–446.
- (16) Schmidt, T.; Wälti, M. A.; Baber, J. L.; Hustedt, E. J.; Clore, G. M. Long Distance Measurements up to 160 Å in the GroEL Tetradecamer Using Q-Band DEER EPR Spectroscopy. *Angew. Chem., Int. Ed.* **2016**, *55*, 15905–15909.
- (17) Meyer, V.; Swanson, M. A.; Clouston, L. J.; Boratyński, P. J.; Stein, R. A.; Mchaourab, H. S.; Rajca, A.; Eaton, S. S.; Eaton, G. R. Room Temperature Distance Measurements of Immobilized Spin Labeled Protein by Double Electron–Electron Resonance Spectroscopy. *Biophys. J.* **2015**, *108*, 1213–1219.
- (18) Rajca, A.; Kathirvelu, V.; Roy, S. K.; Pink, M.; Rajca, S.; Sarkar, S.; Eaton, S. S.; Eaton, G. R. A Spirocyclohexyl Nitroxide Amino Acid Spin Label for Pulsed EPR Spectroscopy Distance Measurements. *Chem. Eur. J.* **2010**, *16*, 5778–5782.
- (19) Kirilyuk, I. A.; Polienko, Y. F.; Krumkacheva, O. A.; Strizhakov, R. K.; Gatilov, Y. V.; Grigor'ev, I. A.; Bagryanskaya, E. G. Synthesis of 2,5-Bis(spirocyclohexane)-Substituted Nitroxides of Pyrroline and Pyrrolidine Series, Including Thiol-Specific Spin Label: An Analogue of MTSSL with Long Relaxation Time. *J. Org. Chem.* **2012**, 77, 8016–8027.
- (20) Kuzhelev, A. A.; Strizhakov, R. K.; Krumkacheva, O. A.; Polienko, Y. F.; Morozov, D. A.; Shevelev, G. Y.; Pyshnyi, D. V.; Kirilyuk, I. A.; Fedin, M. V.; Bagryanskaya, E. G. Room-temperature electron spin relaxation of nitroxides immobilized in trehalose: Effect of substituents adjacent to NO-group. *J. Magn. Reson.* **2016**, *266*, 1–7.
- (21) Eaton, S. S.; Rajca, A.; Yang, Z.; Eaton, G. R. Azaadamantyl nitroxide spin label: complexation with  $\beta$ -cyclodextrin and electron spin relaxation. *Free Radical Res.* **2018**, *52*, 319–326.
- (22) Yang, Z.; Stein, R. A.; Ngendahimana, T.; Pink, M.; Rajca, S.; Jeschke, G.; Eaton, S. S.; Eaton, G. R.; Mchaourab, H. S.; Rajca, A. Supramolecular Approach to Electron Paramagnetic Resonance Distance Measurement of Spin-Labeled Proteins. *J. Phys. Chem. B*, **2020**, *124*, 3291–3299.
- (23) Morozov, D. A.; Kirilyuk, I. A.; Komarov, D. A.; Goti, A.; Bagryanskaya, I. Y.; Kuratieva, N. V.; Grigor'ev, I. A. Synthesis of a Chiral *C*<sub>2</sub>-Symmetric Sterically Hindered Pyrrolidine Nitroxide Radical via Combined Iterative Nucleophilic Additions and Intramolecular 1,3-Dipolar Cycloadditions to Cyclic Nitrones. *J. Org. Chem.* **2012**, 77, 10688–10698.
- (24) Huang, S.; Paletta, J. T.; Elajaili, H.; Huber, K.; Pink, M.; Rajca, S.; Eaton, G. R.; Eaton, S. S.; Rajca, A. Synthesis and Electron Spin Relaxation of Tetracarboxylate Pyrroline Nitroxides. *J. Org. Chem.* **2017**, *82*, 1538–1544.
- (25) Yu, C.-J.; Graham, M. J.; Zadrozny, J. M.; Niklas, J.; Krzyaniak, M. D.; Wasielewski, M. R.; Poluektov, O. G.; Freedman, D. E. Long Coherence Times in Nuclear Spin-Free Vanadyl Qubits. *J. Am. Chem. Soc.* **2016**, *138*, 14678–14685.
- (26) Reboul, M. Oxede de Propylene Normal et Poluoxypropylenes. *Ann. Chim. (Paris)* **1878**, *14*, 495–497.
- (27) Carreira, E. M.; Fessard, T. C. Four-Membered Ring-Containing Spirocycles: Synthetic Strategies and Opportunities. *Chem. Rev.* **2014**, *114*, 16, 8257–8322.
- (28) Bull, J. A.; Croft, R. A.; Davis, O. A.; Doran, R.; Morgan, K. F. Oxetanes: Recent Advances in Synthesis, Reactivity, and Medicinal Chemistry. *Chem. Rev.* **2016**, *116*, 12150–12233.

- (29) Burkhard, J. A.; Wuitschik, G.; Rogers-Evans, M.; Müller, K.; Carreira, E. M. Oxetanes as Versatile Elements in Drug Discovery and Synthesis. *Angew. Chem. Int. Ed.* **2010**, *49*, 9052–9067.
- (30) Edward, J. T.; Farrell, P. G.; Shahidi, F. Partial molar volumes of organic compounds in water. Part 1. Ethers, ketones, esters and alcohols. *J. Chem. Soc., Faraday Trans.* 1, **1977**, *73*, 705–714.
- (31) Moore, J. C.; Battlno, R.; Rettlch, T. R.; Handa, Y. P.; Wilhelm, E. Partial molar volumes of gases at infinite dilution in water at 298.15 K. *J. Chem. Eng. Data* **1982**, *27*, 22–24.
- (32) Berthelot, M.; Besseau, F.; Laurence, C. The hydrogen-bond basicity pK(HB) scale of peroxides and ethers. *Eur. J. Org. Chem.* **1998**, *5*, 925–931.
- (33) Laurence, C.; Brameld, K. A.; Graton, J.; Le Questel, J.-Y. Renault, E. The pK(BHX) Data-base: Toward a Better Understanding of Hydrogen-Bond Basicity for Medicinal Chemists. *J. Med. Chem.* **2009**, *52*, 4073–4086.
- (34) Besseau, F.; Laurence, C.; Berthelot, M. Hydrogen-bond basicity of esters, lactones, and carbonates. *J. Chem. Soc., Perkin Trans.* 2 **1994**, 485–489.
- (35) Zaytseva, E. V.; Mazhukin, D. G. Spirocyclic Nitroxides as Versatile Tools in Modern Natural Sciences: From Synthesis to Applications. Part I. Old and New Synthetic Approaches to Spirocyclic Nitroxyl Radicals. *Molecules* **2021**, *26*, 677 (1-60).
- (36) Fjelbyea, K.; Marigo, M.; Clausen, R. P.; Juhl, K. Preparation of Spirocyclic β-Proline Esters: Geometrically Restricted Building Blocks for Medicinal Chemistry. *Synlett* **2016**, *28*, 231–234.
- (37) Griggs, S. D.; Thompson, N.; Tape, D. T.; Fabrea, M.; Clarke, P. A. Synthesis of highly substituted 2-spiropiperidines. *Org. Biomol. Chem.* **2018**, *16*, 6663–6674.
- (38) Carlock, J. T.; Mack, M. P. A mild quantitative method for the synthesis of variety heterocyclic systems. *Tetrahedron Lett.* **1978**, *52*, 5153–5156.
- (39) Kaboudin, B.; Haghighat, H.; Yokomatsu, T. Studies on the Synthesis of Novel Four-Membered Cyclic Oxaphosphetanes via Intramolecular Mitsunobu Reaction of Bishydroxyalkylphosphinic Acids. *Synlett* **2016**, *27*, 1537–1540.
- (40) Payne, G. B.; Williams, P. H., Reactions of Hydrogen Peroxide. VI. Alkaline Epoxidation of Acrylonitrile. *J. Org. Chem.* **1961**, *26*, 651–659.

- (41) Rauckman, E. J.; Rosen, G. M.; Abou-Donia, M. B. Improved Methods for the Oxidation of Secondary Amines to Nitroxides. *Synth. Commun.* **1975**, *5*, 409–413.
- (42) Luger, P.; Buschmann, J. Oxetane: The First X-Ray Analysis of a Nonsubstituted Four-Membered Ring. *J. Am. Chem. Soc.* **1984**, *106*, 7118–7121.
- (43) Cremer, D.; People, J. A. General definition of ring puckering coordinates. *J. Am. Chem. Soc.* **1975**, *97*, 1354–1358.
- (44) Frisch, M. J.; Trucks, G. W.; Schlegel, H. B.; Scuseria, G. E.; Robb, M. A.; Cheeseman, J. R.; Scalmani, G.; Barone, V.; Petersson, G. A.; Nakatsuji, H.; Li, X.; Caricato, M.; Marenich, A. V.; Bloino, J.; Janesko, B. G.; Gomperts, R.; Mennucci, B.; Hratchian, H. P.; Ortiz, J. V.; Izmaylov, A. F.; Sonnenberg, J. L.; Williams-Young, D.; Ding, F.; Lipparini, F.; Egidi, F.; Goings, J.; Peng, B.; Petrone, A.; Henderson, T.; Ranasinghe, D.; Zakrzewski, V. G.; Gao, J.; Rega, N.; Zheng, G.; Liang, W.; Hada, M.; Ehara, M.; Toyota, K.; Fukuda, R.; Hasegawa, J.; Ishida, M.; Nakajima, T.; Honda, Y.; Kitao, O.; Nakai, H.; Vreven, T.; Throssell, K.; Montgomery, J. A., Jr.; Peralta, J. E.; Ogliaro, F.; Bearpark, M. J.; Heyd, J. J.; Brothers, E. N.; Kudin, K. N.; Staroverov, V. N.; Keith, T. A.; Kobayashi, R.; Normand, J.; Raghavachari, R.; Rendell, A. P.; Burant, J. C.; Iyengar, S. S.; Tomasi, J.; Cossi, M.; Millam, J. M.; Klene, M.; Adamo, C.; Cammi, R.; Ochterski, J. W.; Martin, R. L.; Morokuma, K.; Farkas, O.; Foresman, J. B.; Fox, D. J. Gaussian 16, Revision A.03; Gaussian, Inc.: Wallingford, CT, 2016.
- (45) Chan, S. I.; Zinn, J.; Gwinn, W. D. Trimethylene Oxide. II. Structure, Vibration-Rotation Interaction, and Origin of Potential Function for Ring-Puckering Motion. *J. Chem. Phys.* **1961**, *34*, 1319–1329.
- (46) Rayón, V. M.; Sordo, J. A. Pseudorotation motion in tetrahydrofuran: An ab initio study. *J. Chem. Phys.* **2005**, *122*, 204303.
- (47) Gerson, F.; Huber, W. Electron Spin Resonance Spectroscopy of Organic Radicals, Wiley-VCH, Weinheim, 2003, pp. 49–82.